International Journal of Chemical and Physical Sciences, ISSN:2319-6602
IJCPS Vol. 4 Special Issue ETP – 2015
www.ijcps.org

Synthesis and Characterization of Ni-Cu-Zn Ferrite Materials by Auto Combustion Technique

V. V. AWATI[1]

[1]Department of Physics, C. T. Bora College, Shirur, Pune 412 210, Maharashtra, India
e-mail: vidyadharawati@gmail.com

Abstract

Nanoparticles of $Ni_xCu_{0.1}Zn_{(0.9-x)}Fe_2O_4$ (X = 0.2) were prepared via sol-gel auto combustion method. Structural, morphological, electrical and magnetic properties of nano-crystalline ferrite powders have been investigated by using XRD, FT-IR, FE-SEM, TEM and Hysteresis Tracer. The mean particle size was found to increase from 45 nm to 60 nm by increasing sintering temperature from 400°C to 700°C. The FT-IR spectra of the synthesized nanocrystal confirmed the formation of the spinel structure. The FE-SEM and TEM images showed homogeneous and well distributed crystallized grains of ferrite material. The direct current (DC) resistivity was found to increase from 0.0015 x 10^{10} ohm-cm for as prepared sample to 430.33 x 10^{10} ohm-cm for sample sintered at 700°C. The DC resistivity studies explained the conductivity mechanism. The saturation magnetization was found to be varying from 46.520 emu/g for as prepared sample to 6.700 emu/gm for samples sintered at 700°C. This was credited to the densification and grain growth of prepared ferrites. The optimized electric and magnetic properties indicated that these types of nanoferrites can be used for device fabrication such as multi-layer chip inductors (MLCI's) and for high frequency applications.

Keywords: Nanoparticles; Sol-gel method; FE-SEM; Electrical properties, Magnetic measurements.

Introduction

The fields of ferrites have attracted main attention of scientific research community due to their refreshing properties and technological application in nanomaterial scale. The electric and magnetic behaviors are found to be interesting in comparison with their bulk counterparts [1]. Their electrical and magnetic properties are affected by the type of the substituent, microstructure, chemical composition and method of preparation [2, 3]. The ferrites are commonly prepared by ceramic technique, which involves high temperature sintering with prolong heating. This method produces particles of coarse nature. The ceramic method has some inherent drawbacks and do not produce particles of small sizes of the order of nanometer. In the recent years, nanosize spinel ferrite particles received a considerable attention because of their interesting magnetic properties [4]. It is found that when the particle diameter reduce to nanometer dimension spinel ferrite particles may exhibit super paramagnetic behavior, which is of great interest from the point of view of their applications [5]. Spinel ferrites are compounds of iron oxides and some transition metal oxides and they exhibit important electrical and magnetic properties, which made them extensively useful in technological and industrial applications such as magnetic storage in

microwave devices [6, 7]. The chemical composition method of synthesis, nature of dopant, site preference of dopants etc. parameters strongly influences the structural, electrical and magnetic properties of spinel ferrites [8, 9]. Various substituents of magnetic and nonmagnetic nature like Ni, Zn, Al, etc. have been incorporated in ferrite to modify their properties. In the present study, effect of nickel substitution to copper-zinc ferrite on structural, micro-structural and infrared properties of nanocrystalline Ni-Cu-Zn ferrite synthesized by sol-gel auto combustion are reported.

Experimental Work

Preparation of Samples

The nanoparticles of $Ni_xCu_{0.1}Zn_{(0.9-x)}Fe_2O_4$ (x = 0.2) were devised by using sol-gel auto combustion method from reagent grade constituents namely nickel nitrate, copper nitrate, zinc nitrate and ferric nitrate provided by Merck Company, Germany. The ferrite powders were incurred through a procedure as described below.

Sol-formation

The stoichiometric amount of metal nitrates and citric acid was dissolved into de-ionized water to form a mixed solution. Homogenous distribution and separatism of the metal ions were achieved by the use of citric acid. The pH value of the solution was preserved at 7.0 by drop wise addition of ammonia solution in order to boost up the reaction. The solution was constantly stirred using a magnetic stirrer. The condensation reaction took place between the adjoining metal nitrates and the molecules of citrates yielding a polymer precursor in colloidal dimensions known as sol.

Gel- formation

The obtained sol was heated at 100 ^{0}C on a magnetic stirrer to condensate into a xerogel.

Powder formation

An increase of temperature upto 200 ^{0}C led to the ignition of the dry gel and a loose ferrite nanocrystalline powder was obtained through the burning of gel in a self-propagating combustion manner. During the combustion process, exothermic decomposition of a oxido-reduction mixture of metal nitrates and citric acid took place along with the removal of gases such as CO, H_2O, and CO_2 etc.

Annealing

The as-prepared powder samples were then annealed for 3 h at 400 ^{0}C and 700 ^{0}C in order to enhance the crystallinity. Also the as-prepared ferrite mass was pressed in the form of pellets of 10 mm diameter with the help of hydraulic press by applying pressure of 3 ton for 3 minute. These pellets were sintered at 300 ^{0}C for 2 h in air medium.

Characterization

X-ray diffractometer (Model Bruker D8), with CuKα radiation (λ=1.5405 Å) was used for obtaining XRD patterns. The lattice parameter and crystallite (grain) size of the prepared samples were calculated from the XRD data. Fourier transform infrared spectroscopy (FT-IR) transmittance spectra of prepared ferrite nanoparticles were recorded in the wavenumber range of 400 to 4000 cm^{-1} by using MAGNA 550, Nicolet Instruments Corporation, Madison, WI, USA. The scanning electron microscope (SEM) JEOL JSM -6360A was used to study the morphology and to estimate grain size. The electrical resistivity measurements were carried out by using two probe method at room temperature. Hysteresis Tracer was employed to study the magnetic properties of the samples in the field of 10 kOe at room temperature.

Results and Discussions

Structural Analysis

The XRD patterns of $Ni_xCu_{0.1}Zn_{(0.9-x)}Fe_2O_4$ (x = 0.2) ferrite are shown in Figure 1. The most intense peaks in all specimens indexed as (220), (311), (222), (400), (422), (511), (440) are found to match well with single phase cubic spinel. XRD patterns have confirmed the spinel structure for all the samples. These diffraction peaks demonstrate the formation of ferrite phase in all samples [10]. The average crystallite size for each composition was calculated from the (311) plane using Scherrer formula [11]. The value of crystallite size and lattice parameters deducted from the X-ray data are summarized in Table 1 along with other structural parameters. The lattice parameter and crystallite size was found to increase with annealing temperature, which is in agreement with TEM data. These values are in the range of 45 to 60 nm.

Table 1. Data for lattice parameter, grain size, X-ray density and theoretical density of $Ni_xCu_{0.1}Zn_{(0.9-x)}Fe_2O_4$ (c = 0.2) nanoferrites calculated from XRD data

Particulars	**As prepared**	**at 400°C**	**at 700°C**
Lattice parameter (a) Å	8.312	8.3624	8.371
Grain size (d) nm	45	51	60
X-ray density (D_{hkl}) gm/cc	5.5435	5.4443	5.4271
Theoretical density (D_x) gm/cc	18.390	45.224	81.632
Tetrahedral Ionic radii (r_A) A°	0.4495	0.4794	0.4623
Octahedral ionic radii (r_B) A°	0.728	0.7625	0.7428
Bond length on tetrahedral (A-O) A°	1.8059	1.8295	1.8124
Bond length on octahedral (B-O) A°	2.078	2.1125	2.092
Hopping length on tetrahedral (L_A) A°	3.5992	3.6590	3.624
Hopping length on tetrahedral (L_B) A°	2.9387	2.9816	2.9596

The observed lattice parameter and specific indices are characteristic of spinel structure and confirm the formation of cubic spinel structure in ferrite [12 - 14].

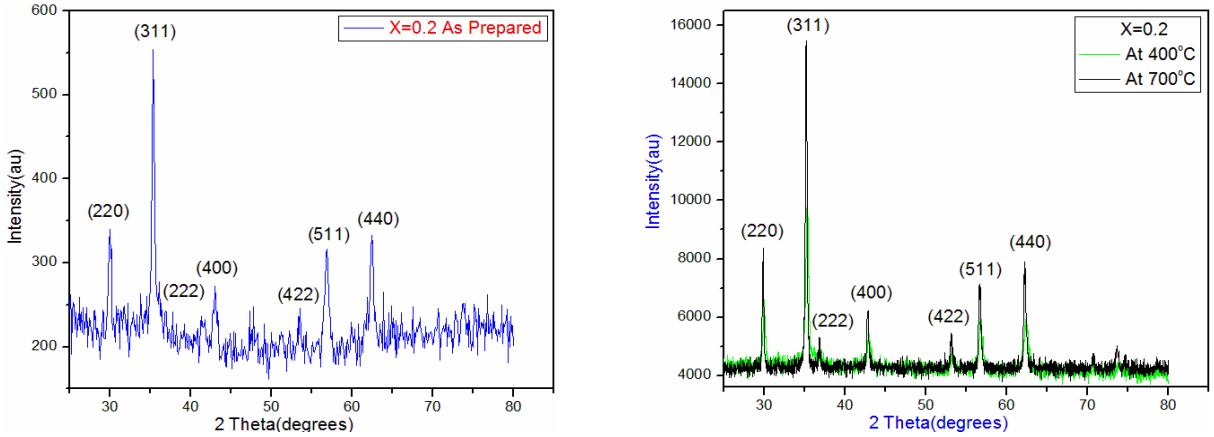

(a) (b)

Figure 1. XRD patterns of samples of $Ni_xCu_{0.1}Zn_{(0.9-x)}Fe_2O_4$ (x = 0.2) nanoferrite

The FTIR study (Figure 2) shows absorption at 3430, 1637, 1450 - 1650, 1387, 555, 442 and 375 - 385 cm^{-1}. In present IR spectrum of the sample, the bands observed at 3425 cm^{-1} and 1622 cm^{-1} are broad and they indicate the presence of water of crystallization in sample. Furthermore, absorption bands arise in the region between 1450 - 1650 cm^{-1} and 1010 - 1210 cm^{-1} are related to the vibration of a C-O bond. This spectrum represent characteristic features of ferro spinels, and bands are attributed to the stretching vibration due to interactions between the oxygen atom and the cations in tetrahederal and octahederal sites respectively. The behavior is attributed to the stretching of Fe-O bonds on substitution of Ni ions. The FTIR results clearly indicates that Ni ion occupy the tetrahederal sites in the Cu-Zn matrix of nanoparticles. Figure 3(a), 3(b) and 3(c) show the Scanning electron micrograph (SEM) images of $Ni_xCu_{0.1}Zn_{(0.9-x)}Fe_2O_4$ (x = 0.2) ferrites for as prepared and samples sintered at 400 ^{0}C and 700 ^{0}C.

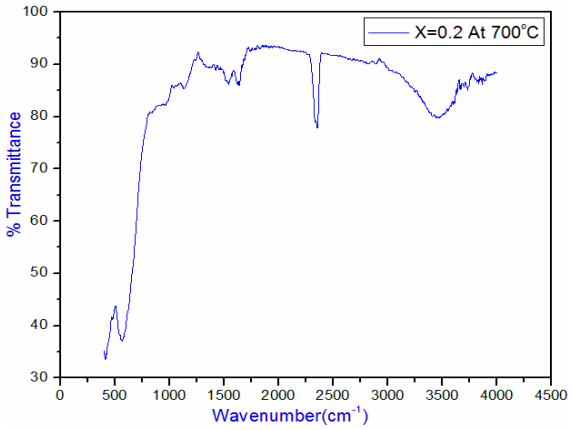

Figure 2. FTIR spectruma of samples of $Ni_xCu_{0.1}Zn_{(0.9-x)}Fe_2O_4$ (x = 0.2) nanoferrite

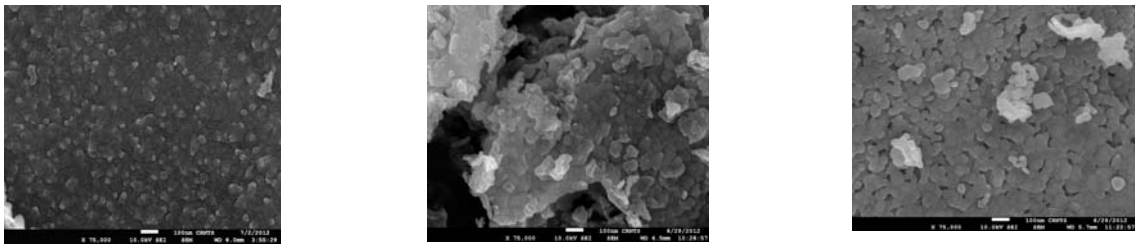

(a) (b) (c)

Figure 3. SEM of $Ni_xCu_{0.1}Zn_{(0.9-x)}Fe_2O_4$ (x = 0.2) for (a) as-prepared (b) at 400 ^{0}C (c) at 700 ^{0}C

The micrographs show largely agglomerated nanoparticles of the sample powder. Such aggregate formation and border size distribution are characteristics of mechanically activated nano-sized particle. It is observed that the synthesized samples have large clusters of ferrites formed by assembling of small particles of nearly consistent in size with spherical nature. Similar results are reported for Cu substituted Mn-Zn soft nanoferrites by Anwar et al. [15]. The particles were observed as uniform grains confirming the crystalline structure of copper zinc ferrite, which were detected by the XRD outline. The formation of Fe_2O_3 was chemically favored during the heating. Whereas, the final reaction was completed during the sintering, where the pores between the particles were removed and combined with growth, and strong bonds between the adjacent particles were formed. Each grain is formed by group of a number of nanocrystals. The samples with spherical, uniform and cohesion of grains are due to magnetic attraction. Figure 4(a, b), Figure 5(a, b) and, Figure 6(a, b) show TEM micrographs of the synthesized nanoparticles along with the selected area electron diffraction (SAED) patterns for pure and doped Ni-Cu-Zn ferrites for as prepared and samples at annealed 400 ^{0}C and 700 ^{0}C.

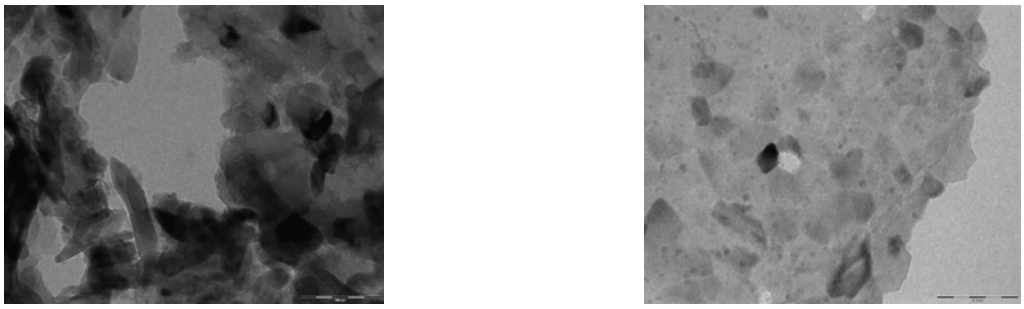

(a) (b)

Figure 4. TEM microphotograph of as prepared $Ni_xCu_{0.1}Zn_{(0.9-x)}Fe_2O_4$ (x = 0.2) ferrite

According to figure, the particle are seen to be in spherical form with crystallite size of 45 to 68 nm and electron diffraction patterns confirm the spinel structure of ferrite with several lines (220), (311), (400), (511) and (440) depicted from TEM data. In the SAED image of synthesized nanoparticle, distinct rings that confirm good crystallinity are clear visible. The observed crystallographic d values of 2.51 A^o corresponds to the lattice space of (311) plane of the Ni-Cu-Zn ferrite system.

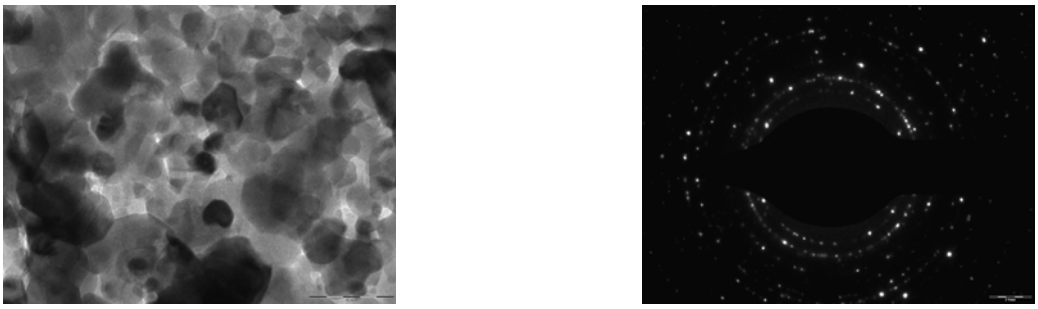

(a) (b)

Figure 5. TEM microphotograph of $Ni_xCu_{0.1}Zn_{(0.9-x)}Fe_2O_4$ (x = 0.2) ferrite annealed at 400 ^{0}

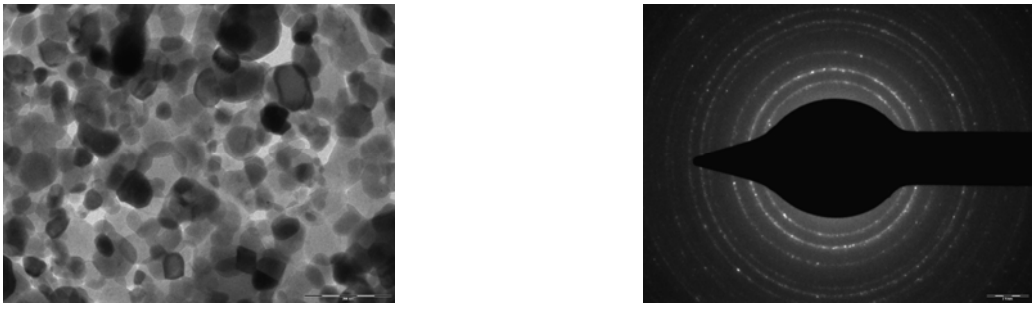

(a) (b)

Figure 6. TEM microphotograph of $Ni_xCu_{0.1}Zn_{(0.9-x)}Fe_2O_4$ (x = 0.2) ferrite annealed at 700 ^{0}

Resistivity measurements

DC resistivity of all samples was measured using a two-probe method fig. 7(a,b). It is observed that DC resistivity shows a linear increase with sintering temperature as shown in Table 2 [16]. This variation is explained by the location of the cations in the spinel ferrite. The observed increase in resistivity can be understood by considering the hopping mechanism $Fe^{2+} \leftrightarrow Fe^{3+}$[17-18].

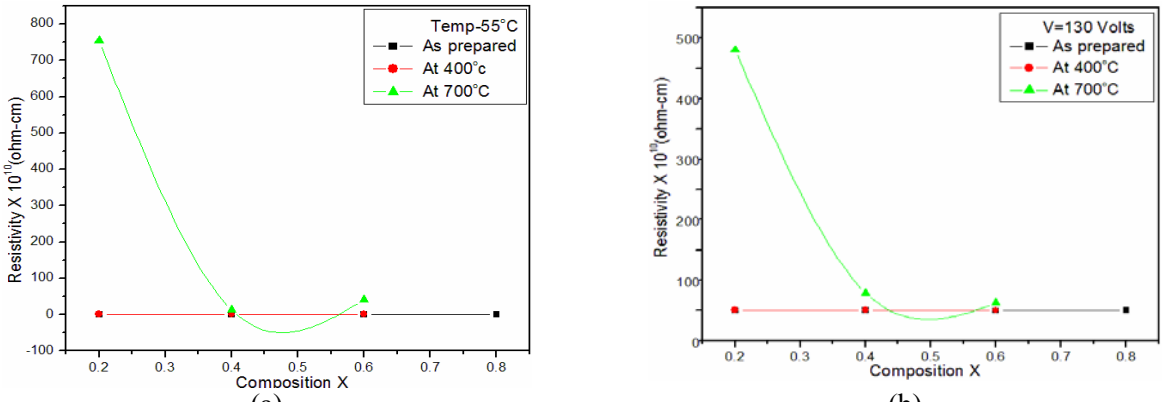

(a) (b)

Figure 7. Compositional dependence DC resistivity in $Ni_xCu_{0.1}Zn_{(0.9-x)}Fe_2O_4$ (X = 0.2)

The increase in Ni^{2+} ions at the B site leads to replacement of Fe^{3+} ions at B site, leading to a decrease of ferrous ions formed. Though the Ni^{2+} ions do not participate in the conduction mechanisms, they limit the degree of $Fe^{2+} \leftrightarrow Fe^{3+}$ transfer, thereby obstructing electron hopping and resulting in an

increase in resistivity. The similar nature of resistivity has been described earlier [19]. The conduction in the samples is due to grain boundaries. The high values of DC electrical resistivity support this result.

Table 2. Resistivity and conductivity of $Ni_xCu_{0.1}Zn_{(0.9-x)}Fe_2O_4$ (X=0.2) nano-ferrite materials.

Sample	**Temp. (^oC)**	**Resistivity x 10^{10} (ohm-cm)**	**Conductivity x 10^{-10} $(ohm\text{-}cm)^{-1}$**
As prepared	20	0.0026	384.61
	30	0.0026	384.61
	50	0.0010	1000.00
at 400^0C	20	0.7937	1.2599
	30	0.8082	1.2373
	50	0.5611	1.7822
at 700^oC	20	88.38	0.0113
	30	1142.60	0.0008
	50	754.22	0.0013

Magnetic Properties

Magnetic hysteresis loops plotted for $Ni_xCu_{0.1}Zn_{(0.9-x)}Fe_2O_4$ (X = 0.2) nanoferrites is shown in Fig. 8. It was observed that the magnetization increases rapidly in the low field area as shown in the Table 3. However, it could not reach to the saturation state by applying high magnetic field. Similar observations at room temperature magnetization have been reported by Koseoglu et al. [20], and Wang et al. [21]. Superparamagnetic 'S' shaped hysteresis curves are obtained for all ferrite structures. The saturation magnetization M_s was found by extrapolating M_s versus 1/H plot to 1/H = 0. It was observed that the value of M_s decreases with sintering temperature and become 6.700 emu/g.

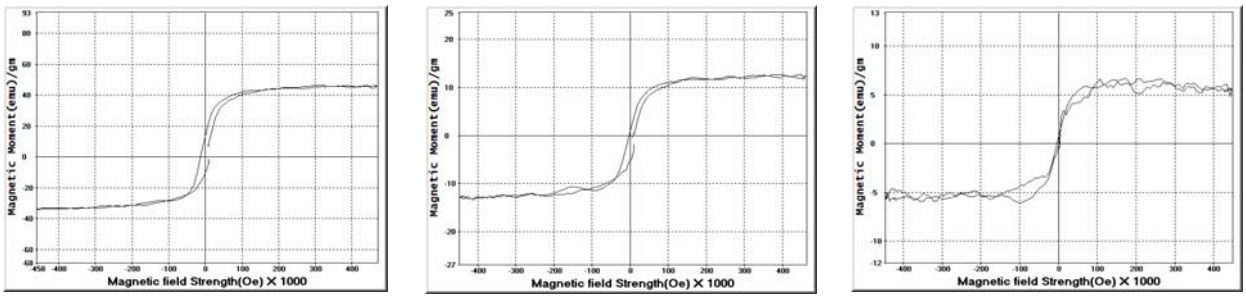

(a) (b) (c)

Figure 8. Magnetic hysteresis loops of $Ni_xCu_{0.1}Zn_{(0.9-x)}Fe_2O_4$ (X = 0.2) nano ferrites

The concentration of Ni and sintering temperature impresses on the resultant magnetization [22]. The decrement of M_s in prepared material was assigned to the existence of random canting of particles caused by antiferromagnetic exchange interactions due to asymmetry of these spins [23]. The high values

of coercivity of the order of 3336.45 Oe indicates pinning of magnetization at the grain boundaries. The presence of Ni^{2+} ion at tetrahederal sites produces anisotropy.

Table 3. Magnetic properties of $Ni_xCu_{0.1}Zn_{(0.9-x)}Fe_2O_4$ (X = 0.2) nano ferrites.

Sample	**M_s (emu/gm)**	**M_r (emu/gm)**	**H_c (Oe)**	**M_r/M_s**
As prepared	46.5205	19.8364	3336.45	0.4264
at 400^0C	12.7325	3.4516	2010.03	0.2710
at 700^0C	6.700	1.300	437.817	0.1940

Conclusions

The experimental investigation shows how properties of spinel Copper-Zinc ferrites are affected by doping of Nickel. We have prepared these samples through the sol-gel method and performed various structural, dielectric and magnetic measurements on them with sintering temperatures at 400 ^{0}C and 700 ^{0}C. The conclusions are as follows:

a) The broad XRD peak indicates the formation of nanoferrites. The observed lattice parameter and specific indices are characteristics of spinel structure with no any indentifying or secondary peaks.
b) The FTIR spectrum of the synthesized nanocrystal confirms the formation of the spinel structure.
c) The SEM and TEM results of the sintered samples show that the grain boundary grew as temperature increases.
d) The hopping of electrons between Fe^{3+} and Fe^{2+} as well as the hole hopping between nickel ions are found to be responsible for the conduction mechanism.
e) For all samples, an 'S' like shape hysteresis curve was observed. The saturation magnetization (M_s) value is 6.700 emu/g at 700^{o}C.

The prepared ferrite materials have high DC resistivity and low saturation magnetization. These results are capable for the use of these materials in high frequency functional device applications.

Acknowledgement

The author acknowledges Prof. N.S. Nikam, Principal, C. T. Bora College, Shirur, Dist. Pune for laboratory facilities, Director, BCUD, SPPU for financial assistance, SAIF, IIT, Bombay, Powai for characterization facilities, Department of Physics, Abasaheb Garware College, Pune for magnetic characterization.

References

[11]W. C. Kim, S. J. Kim, S. W. Lee, and C. S. Kim, "Growth of ultrafine NiCuZn ferrite and magnetic property by sol-gel method," J. Magn. Magn. Mater, vol. 226, pp. 1418 - 1420, 2001.

[12] C. Kittle, "Domain theory and the dependence of the coercive force of fine ferromagnetic powders on particle size," Phys. Rev. B, vol. 73, pp. 810 - 811, 1948.

[13] W. Y. Lucas, J. W. Moon, C. Rawn, L. J. Lane, A. Rondinone, J. R. Tompson, B. C. Chakoumakis, and T. J. Phelps, "Magnetic properties of bio-synthesized zinc ferrite nanoparticles," J. Magn. Magn. Mater., vol. 323, pp. 3043 - 3048, 2011.

[14] K. Y. Kim, W. S. Kim, Y. D. Ju, and H. J. Jung, "Effect of addition of the Cu-Fe_2O_3 system on the electromagnetic wave absorbing properties of sintered ferrite," J. Mater. Aci. vol. 27, pp. 4741 - 4745, 1992.

[15]P. Hu, D. -A. Pan, X. F. Wang, S. -G. Zhag, and A. A. Volinsky, "Fuel additives and heat treatment effect on nanocrystalline zinc ferrite phase composition," J. Magn. Magn. Mater., vol. 323, pp. 569 - 573, 2011.

[16] E. C. Snelling, Soft ferrites: Pro. & Appl., London ILIFFEE Book Ltd., pp. 26, 1969.

[17]M. Srivastava, S. Chaubey, and A. K. Ojha, "Investigation on size dependent structural and magnetic behavior of nickel ferrite nanoparticles prepared by sol-gel and hydrothermal method," Mater. Chem. Phys., vol. 118, pp. 174 - 180, 2009.

[18] W. C. Kim, S. J. Kim, S. W. Lee, and C. S. Kim, "Growth of ultrafine NiZnCu ferrite and magnetic properties by a sol-gel method," J. Magn. Magn. Mater., vol. 226, pp. 1418 - 1420, 2001.

[19]J. Mohapatra, A. Mitra, D. Bahadur, and M. Aslam, "Controlled fabrication of MFe_2O_4 (M = Mn, Fe, Co, Ni and Zn) nanoparticles and their magnetic properties," Cryst. Eng. Comm., vol. 15, pp. 524, 2013.

[20] P. Bayliss, and D. K. Smith, Mineral Powder Diffraction File, JCPDS, USA, 1986.

[21] B. D. Cullity, "Elements of X-ray diffraction," Addison Wesley Publish. Co., England, pp. 42, 1967.

[22] A. Thakur, P. Mathur, and M. Singh, "Controlling the properties of Mn-Zn ferrites at high frequency by substituting In^{3+} and Al^{3+} ions," Ind. J. Pure Appl. Phys., vol. 46, pp. 43, 2008.

[23] C. M. B. Henderson, J. M. Charnock, and D. A. Plant, "Cation occupancies in Mg, Co, Ni, Zn, Al-ferrite spinels: a multi-element EXAFS study," J. Phys. Condens. Matter, vol. 19, pp. 076214, 2007.

[24] A. A. Sattar, H. M. El. Sayed, and M. M. El-Tabey, "The effect of Al substitution on structure and electrical properties of Mn-Ni-Zn ferrites," J. Mater. Sci., vol. 40, pp. 4873, 2005.

[25] H. Anwar, and A. Maqsood, "Structural, magnetic and electrical properties of Cu substituted Mn-Zn soft nanoferrites," J. Supercond. Nov. Magn., vol. 25, pp. 1913, 2012.

[26] M. U. Islam, T. Abbas, S. B. Niazi, Z. Ahmed, S. Saben, and M. A. Choudhary, "Electrical behavior of fine particle, co-precipitation prepared Ni-Zn ferrites," Solid State Commun., vol. 130**,** issue 5, pp. 353 - 356, 2004.

[27] G. Joshi, A. Khot, and S. Sawant, "Revised values of effective ionic radii," Solid State Commun., vol. 65, 1593, 1998.

[28] M. E. Shabashy, "DC electrical properties of Ni-Zn ferrites, J. Magn. Magn. Mater., vol. 172, issue 1 - 2, pp. 188 - 192, 1997.

[29] U. Ghazanfar, S. A. Siddiqui, and G. Abbas, "Study of room temperature dc resistivity in comparison with activation energy and drift mobility of Ni-Zn ferrite," Mater. Sci. & Engg. B, vol. 118 issue 1 - 3, 132 - 134, 2005.

[30] Y. Koseoglu, and A. Baykal, "Structural and magnetic properties of $Co_xZn_{1-x}Fe_2O_4$ nanoparticles synthesized by microwave method," Polyhedron, vol. 28, pp. 2887, 2009.

[31] J. Wang, "Magnetic properties of $ZnFe_2O_4$ nanoparticles produced by a low-temperature solid state reaction method," J. Magn. Magn. Mater., vol. 309, pp. 295 2007.

[32] C. Venkataraju, G. Sathishkumar, and K. Sivakumar, "Effect of cation distribution on the structural and magnetic properties of nickel substituted nanosized Mn-Zn ferrites prepared by co-precipitation method," J. Magn. Magn. Mater., vol. 322, pp. 230, 2010.

[33] J. M. D. Coey, "Noncollinear spin structures," Can. J. Phys., vol. 65, pp. 1210, 1987.